

# Photooxidative Generation of Dodecaborate-Based Weakly Coordinating Anions

Jonathan C. Axtell,<sup>\*,†,‡</sup> Marco S. Messina,<sup>†,‡</sup> Ji-Yuan Liu,<sup>§</sup> Daria Galaktionova,<sup>||</sup> Josef Schwan,<sup>⊥</sup> Tyler M. Porter,<sup>#</sup> Miles D. Savage,<sup>†</sup> Alex I. Wixtrom,<sup>†</sup> Arnold L. Rheingold,<sup>#</sup> Clifford P. Kubiak,<sup>#</sup> Jay R. Winkler,<sup>⊥</sup> Harry B. Gray,<sup>\*,⊥,‡</sup> Petr Král,<sup>\*,||,¶,∇</sup> Anastassia N. Alexandrova,<sup>\*,†,‡</sup> and Alexander M. Spokoyny<sup>\*,†,‡</sup>

<sup>†</sup>Department of Chemistry and Biochemistry, University of California, Los Angeles, 607 Charles E. Young Drive East, Los Angeles, California 90095-1569, United States

<sup>‡</sup>California NanoSystems Institute, University of California, Los Angeles, 570 Westwood Plaza, Los Angeles, California 90095-1569, United States

<sup>§</sup>Key Laboratory for Advanced Materials, Center for Computational Chemistry and Research Institute of Industrial Catalysts, School of Molecular Science and Engineering, East China University of Science and Technology, Shanghai 200237, P. R. China

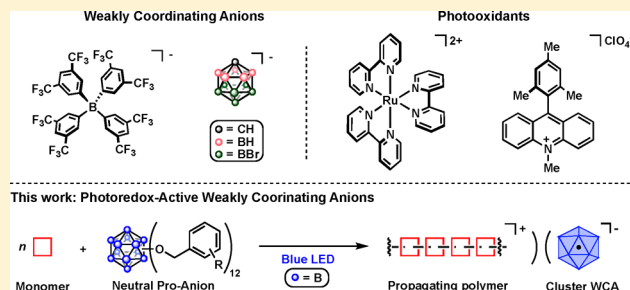
<sup>||</sup>Department of Chemistry, <sup>¶</sup>Department of Physics, and <sup>∇</sup>Department of Biopharmaceutical Sciences, University of Illinois at Chicago, Chicago, Illinois 60607, United States

<sup>⊥</sup>Beckman Institute, California Institute of Technology, Pasadena, California 91115, United States

<sup>#</sup>Department of Chemistry and Biochemistry, University of California, San Diego, 9500 Gilman Drive, La Jolla, California 92093, United States

## Supporting Information

**ABSTRACT:** Redox-active proanions of the type  $B_{12}(OCH_2Ar)_{12}$  [Ar =  $C_6F_5$  (1),  $4-CF_3C_6H_4$  (2),  $3,5-(CF_3)_2C_6H_3$  (3)] are introduced in the context of an experimental and computational study of the visible-light-initiated polymerization of a family of styrenes. Neutral, air-stable proanions 1–3 were found to initiate styrene polymerization through single-electron oxidation under blue-light irradiation, resulting in polymers with number-average molecular weights ( $M_n$ ) ranging from ~6 to 100 kDa. Shorter polymer products were observed in the majority of experiments, except in the case of monomers containing 4-X (X = F, Cl, Br) substituents on the styrene monomer when polymerized in the presence of 1 in  $CH_2Cl_2$ . Only under these specific conditions are longer polymers (>100 kDa) observed, strongly supporting the formulation that reaction conditions significantly modulate the degree of ion pairing between the dodecaborate anion and cationic chain end. This also suggests that 1–3 behave as weakly coordinating anions (WCA) upon one-electron reduction because no incorporation of the cluster-based photoinitiators is observed in the polymeric products analyzed. Overall, this work is a conceptual realization of a single reagent that can serve as a strong photooxidant, subsequently forming a WCA.



## INTRODUCTION

The concept and use of weakly coordinating anions (WCAs) have been known for many years within the chemical community. The unique properties of these species—in particular, their electrochemical and kinetic stability—have been leveraged to isolate highly reactive intermediates and facilitate unique chemical transformations. Applications of WCAs within the polymer community began with important discoveries employing noncoordinating borane anions [e.g.,  $B[3,5-(CF_3)_2C_6H_3]_4^-$  ( $BAR^F$ )] or proanions [e.g.,  $B(C_6F_5)_3$ ] in cationic polymerizations;<sup>1–3</sup> these types of reagents have been reviewed<sup>4</sup> and continue to be developed and applied in different areas of chemistry.<sup>5</sup> More recently, this concept has

been extended to using heterogeneous supports, themselves, as WCAs to activate metal hydride or metal alkyl fragments, generating chemisorbed cationic metal catalysts.<sup>6</sup>

State-of-the-art WCAs, however, are not without their limitations. For example, even (fluoroaryl)borate anions have been shown to react with high-valent metal centers through ring-transfer reactions.<sup>7</sup> Highly Lewis acidic arylboranes, which

**Special Issue:** Celebrating the Year of the Periodic Table: Emerging Investigators in Inorganic Chemistry

**Received:** March 30, 2019

**Published:** June 25, 2019

have been used to generate WCAs in situ, readily form adducts with water<sup>8</sup> and have also been shown to engage in ring-transfer activity.<sup>9</sup> Waldvogel and co-workers recently disclosed an electrochemical study of  $BAr_4$ -based anions and detailed their instability toward arene–arene coupling at strongly oxidizing potentials.<sup>10</sup> Furthermore, many WCAs are introduced as salts, which are often synthetically nontrivial, and the formation of the desired ion pair can be complicated by incomplete salt metathesis or the formation of associated salt adducts.<sup>4</sup> Conceptually, access to WCAs from neutral precursors that can be triggered by external stimuli such as light would potentially ameliorate some of these challenges, although to our knowledge, no photoredox-active weakly coordinating proanions have been reported (Figure 1).

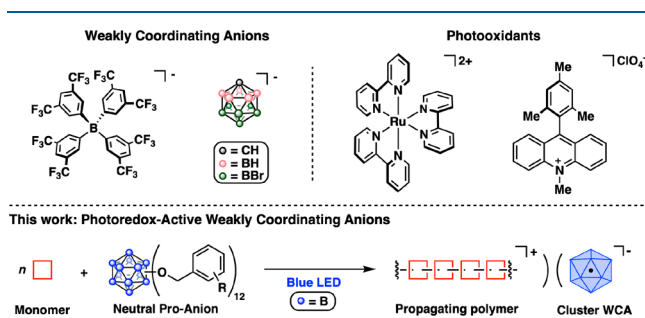


**Figure 1.** Properties of WCAs and photooxidants harnessed simultaneously through the use of perfunctionalized photoredox-active boron cluster proanions.

Perfunctionalized dodecaborane clusters of the type  $B_{12}(OCH_2Ar)_{12}$  (**1**; Ar = Ph,  $C_6F_5$ ) initiate the polymerization of a range of styrenes as well as that of isobutylene.<sup>11</sup> We therefore wondered whether species of this type might breach new chemical space in the context of WCA chemistry.<sup>12</sup> In general, the use of icosahedral boron clusters—typically the monoanionic carba-*closo*-undecaborate,  $[CB_{11}H_{11}]^-$ , and its functionalized derivatives—as WCAs is well-known,<sup>13</sup> and they continue to be used to great effect, as shown, for example, in recent disclosures by Nelson and co-workers.<sup>14</sup> While  $B_{12}(OCH_2Ar)_{12}$  species can be easily isolated as charge-neutral species, upon photoexcitation of certain derivatives with visible light, their extreme photooxidizing behavior [e.g., 2.98 V vs saturated calomel electrode (SCE) for **1**] can activate substrates toward single electron transfer (ET), forming a substrate-based radical cation and a stable, cluster-based radical anion. Here we provide evidence for the WCA behavior of  $[B_{12}(OCH_2Ar)_{12}]^-$ , photooxidatively generated by the reaction of **1–3** with a variety of styrenes under blue-light-emitting-diode (LED) irradiation. This study opens the door to previously unexplored photoredox-active WCAs.

## ■ SYNTHESIS AND SELF-EXCHANGE STUDIES

A hallmark of **1** is the high photooxidizing potential displayed under blue-light irradiation, enabling reactivity toward species of otherwise appreciable oxidative stability. We wondered whether such behavior was general across other  $B_{12}(OCH_2Ar)_{12}$  analogues bearing electron-withdrawing benzyl substituents: we suspected that similarly electron-deficient  $B_{12}(OCH_2Ar)_{12}$  species  $B_{12}(OCH_2-4-CF_3C_6H_4)_{12}$  (**2**)<sup>15</sup> and recently reported  $B_{12}(OCH_2-3,5-(CF_3)_2C_6H_3)_{12}$  (**3**)<sup>16</sup> would be capable of initiating styrene polymerization. Indeed, **2** and **3** also initiate the polymerization of a number of styrene

derivatives (vide infra). Although the syntheses of **1** and **2** are known, we have developed a more general and operationally straightforward protocol for neutral  $B_{12}(OCH_2Ar)_{12}$  species containing electron-withdrawing Ar substituents: while  $FeCl_3$  is a sufficiently strong oxidant to generate **1** and **2**, it is not a strong enough oxidant under identical conditions to generate **3** from  $[B_{12}(OCH_2-3,5-(CF_3)_2C_6H_3)_{12}]^{2-/-}$  ( $[3]^{2-/-}$ ; note that, for  $[#]^{2-/-}$  ( $\# = 1-3$ ), the  $NBu_4^+$  counterion is implied unless otherwise noted); in fact,  $[3]^-$  is generated selectively by the treatment of  $[3]^{2-/-}$  with  $FeCl_3$ .<sup>15</sup> We find that treating  $[B_{12}(OCH_2Ar)_{12}]^{2-/-}$  mixtures of **1–3** with  $NOBF_4$  in  $CH_3CN$  rapidly and cleanly generates the respective oxidized, charge-neutral species (Figure 2A).

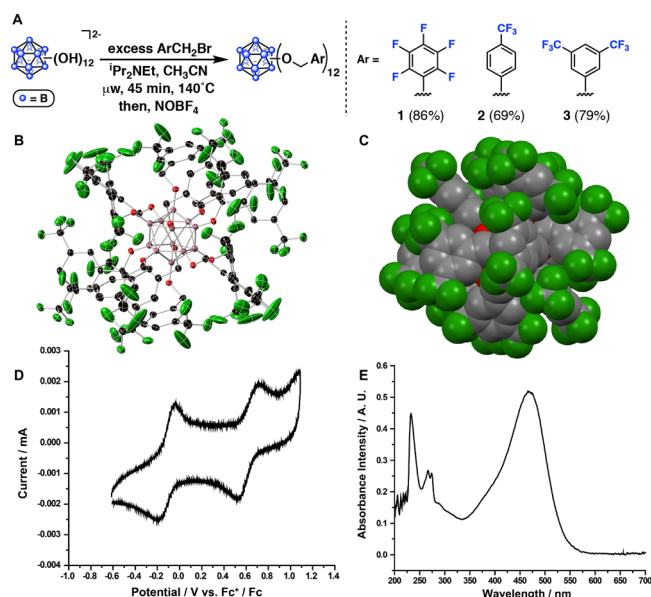


**Figure 2.** (A) Synthetic protocol to generate neutral  $B_{12}(OCH_2Ar)_{12}$  species from  $[B_{12}(OH)_{12}]^{2-}$ . Single-crystal X-ray structure (B; thermal ellipsoids at 50% probability) and space-filling model (C) of dodecaborane **3**. (D and E) Cyclic voltammogram ( $CH_3CN$ ) and UV–visible absorption spectrum ( $CH_2Cl_2$ ) of **3**.

Compound **3** crystallizes from hot toluene (see Figure 2B,C for a single-crystal X-ray structure and a space-filling diagram) and exhibits the most anodically shifted 0/1– redox couple (0.68 V vs  $Fc/Fc^+$ )<sup>15</sup> of any  $B_{12}(OR)_{12}$  species reported to date (Figure 2D); as with other characterized  $B_{12}(OCH_2Ar)_{12}$  species, **3** exhibits a strong absorption in the blue (~450 nm) region (Figure 2E). Bond angles and distances measured for **3** are consistent with structurally characterized *hypercloso*- $B_{12}(OR)_{12}$  species. Importantly, the oxidation reactions generating **1–3** using  $NOBF_4$  can be carried out on gram scales to afford air-stable, neutral dodecaboranes in high yields.

Our ability to cleanly isolate  $[3]^-$  and **3** through the treatment of  $[3]^{2-/-}$  with  $FeCl_3$  and  $NOBF_4$ , respectively, prompted a solution-phase electron-self-exchange study using  $^{19}F$  NMR spectroscopy in order to probe ET kinetics. We anticipated that such a study would shed light on ET between the cluster and substrate during styrene polymerization initiated by photoexcited  $B_{12}(OCH_2Ar)_{12}$ . At temperatures varying from 20 to 60 °C in 1,2-dichloroethane, we recently showed that electron self-exchange between  $[NBu_4][3]$  and **3** is slow on the NMR time scale, with  $k_{ex} < 1.2 \times 10^3 M^{-1} s^{-1}$ .<sup>16</sup>

It is known that electron self-exchange between the 0/1-redox pair in  $\text{Ru}_3\text{O}(\text{OAc})_6(\text{CO})(\text{L})_2$  clusters [where  $\text{L} = 4$ -cyanopyridine, pyridine, or 4-(dimethylamino)pyridine] is highly dependent on the degree of charge density residing on the ancillary pyridyl ligands.<sup>17</sup> Given the encumbering steric profile of pseudospherical 1–3 and considering that the highest occupied molecular orbital (HOMO) of  $[3]^-$  and the lowest unoccupied molecular orbital (LUMO) of ground-state 3 are exclusively boron-cage-based,<sup>16</sup> we attribute this low rate of ET to poor electronic coupling between 3 and  $[3]^-$  in the ground state. However, upon photoexcitation, these species possess oxidizing potentials exceeding 3 V versus SCE (vide infra), resulting in rapid hole transfer to the substrate. Ultimately, these qualities lay the groundwork for the development of sterically and electrochemically tunable neutral reagents that result in the generation of WCAs in situ through visible-light irradiation.

### ■ STYRENE POLYMERIZATION

Our initial polymerization studies<sup>11</sup> with 1 in  $\text{CH}_2\text{Cl}_2$  under blue-LED irradiation revealed good yields for moderate-to-electron-rich styrenes and dispersity values of  $\sim 2$ , which might be expected for uncontrolled carbocationic polymerizations;<sup>18</sup> control experiments showed that these polymerizations do not proceed in the absence of 1 and that radical-based propagation modes are not likely. Interestingly, monomers with *p*-halide substituents displayed very high  $M_n$  and excellent yields, despite the inductively electron-withdrawing nature of the *p*-F and *p*-Cl substituents ( $\sigma_p = 0.06$  and 0.23, respectively<sup>19</sup>), and were unexpected in comparison to other monomers: electronically similar monomers such as styrene [ $\sigma_p(\text{H}) = 0.00$ ] and 3-Cl-styrene [ $\sigma_m(\text{Cl}) = 0.37$ ] gave significantly smaller  $M_n$  values.

In order to better understand these results, we screened a family of vinylarenes with initiators 1–3 in  $\text{CH}_2\text{Cl}_2$  and 1,2-difluorobenzene (Figure 3) to probe generality, i.e., whether

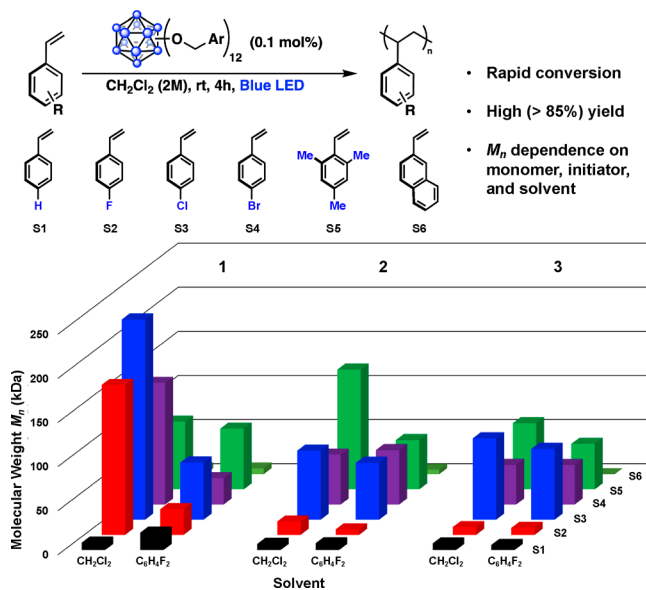


**Figure 3.** Reaction conditions and monomer sets for photoinitiated polymerizations by 1–3. The bar chart depicts  $M_n$  values obtained for all polymerizations and reveals the unusually high  $M_n$  values obtained for S2–S4 in  $\text{CH}_2\text{Cl}_2$  with 1. A numerical summary of these values with corresponding polymer yields can be found in the SI.

other perfunctionalized dodecaborates were also capable of initiating styrene polymerization via visible-light irradiation. Overall, we find that moderate  $M_n$  values are obtained in nearly all cases, consistent with an uncontrolled cationic polymerization involving a counteranion that does not effectively stabilize the cationic chain end:<sup>18a</sup> moderate  $M_n$  values were obtained for S1–S6 in 1,2-difluorobenzene for 1–3 under standard conditions;  $M_n$  values for a given monomer were also consistent for S1–S6 using 2 and 3 in  $\text{CH}_2\text{Cl}_2$ . For 1, while S1, S5, and S6 again displayed comparable  $M_n$  values when initiated in  $\text{CH}_2\text{Cl}_2$ , S2–S4, which contain 4-X ( $\text{X} = \text{F}, \text{Cl}, \text{Br}$ ) substituents, displayed  $M_n$  values over 1 order of magnitude larger than that of in 1,2-difluorobenzene. In most cases, polydispersities range from  $\sim 1.8$  to 2.3 and appear to be independent of the trend observed for polymers generated using 1 and S2–S4 in  $\text{CH}_2\text{Cl}_2$ . Polymer analysis by matrix-assisted laser desorption ionization mass spectrometry did not show incorporation of the initiator in any cases tested (see the Supporting Information (SI) for representative examples); this is consistent with previously obtained inductively coupled plasma mass spectrometry data<sup>11</sup> as well as the general inertness of the dodecaborate counterion in the presence of a reactive cationic chain end. We suggest that the unique distribution of polymer molecular weights based on the solvent, initiator, and monomer indicates both the weakly interacting behavior of the dodecaborate anions with the cationic chain end as well as an easily influenced equilibrium (vide infra) of these interactions from contact ion pairs to more efficiently solvated ion pairs; the location of this equilibrium ultimately determines the resulting  $M_n$  values.

### ■ COMPUTATIONAL ANALYSIS OF PHOTOEXCITATION

Attempts to probe the proposed intermolecular interactions of the perfunctionalized dodecaboranes and a donor molecule (e.g., styrene) spectroscopically prior to ET so far have been unsuccessful, consistent with the short excited-state lifetime ( $\tau = \sim 360$  ps for 1),<sup>11</sup> high excited-state reduction potential, and cluster-based HOMO and LUMO levels of 1–3 in the ground state (vide infra). Therefore, a computational evaluation of both isolated dodecaboranes as well as cluster–monomer interactions was undertaken.

We first initiated a computational study to evaluate the electronic properties of 1–3 as well as select monomers in order to identify qualities that might give rise to the unique performance of 1. First, we investigated whether the generation of high  $M_n$  polymers by 1 resulted simply from the difference in energy between the HOMO of the monomer and the lower energy, cluster-based donor orbital(s) responsible for blue-light absorption. As shown in Figure 4, no clear correlation is observed between the monomer HOMO energy and polymer length for 1 in  $\text{CH}_2\text{Cl}_2$ . We calculated the ionization potentials of three representative monomers (S1, S3, and S5) and found that both in the gas phase and with a  $\text{CH}_2\text{Cl}_2$  solvent model the energies for all three monomers are comparable and scale in the order of  $\text{S1} > \text{S3} > \text{S5}$  (see the SI). In addition, the occupied orbitals involved in the visible-light ( $\sim 450$  nm) absorption in all three initiators have similar parentages (Figure 4B) and oscillator strengths, with absorption maxima that closely reflect measured values (see the SI). This suggests that the donor and acceptor orbitals involved in visible-light absorption are not unique for 1 and therefore cannot, by themselves, explain the inconsistent behavior of 1 in producing polymers of only moderate  $M_n$  compared with 2 or 3 under otherwise identical conditions. Excited-state reduction potentials were estimated for 2 and 3 through fluorescence measurements in perfluorotoluene at 77 K and, in combination with ground-state potentials (which are, in fact, more anodic than 1 for the analogous 0/1-redox couples<sup>15</sup>), are higher than that of 1 ( $\sim 2.98$  V vs SCE<sup>11</sup>), reaching values of  $\sim 3.21$

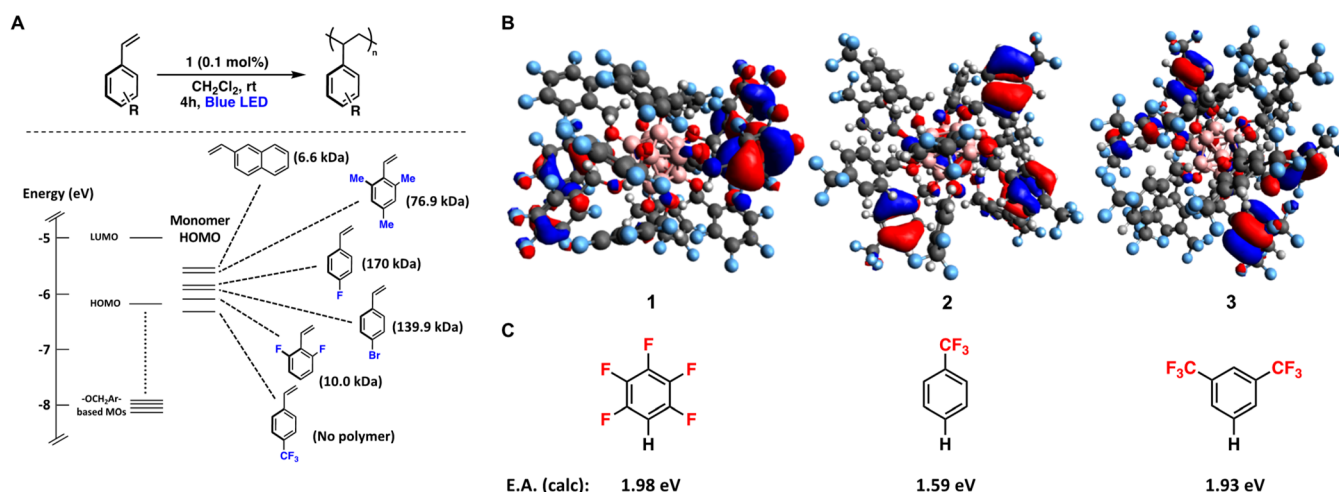


**Figure 4.** (A) Relative energies of vinylarene HOMOs and corresponding  $M_n$  obtained with **1**. (B) Representative donor molecular orbitals of **1–3** that are primarily oxygen-based with some contribution from the benzyl units. (C) Calculated electron affinity values for aryl substituents corresponding to **1–3**.

and  $\sim 3.33$  V versus SCE for **2** and **3**, respectively (see the SI). In addition, electron affinity values for the arene fragments that correspond to **1–3** [ $C_6F_5H$ ,  $C_6H_5CF_3$ , and  $m-(CF_3)_2C_6H_4$ , respectively] have comparable energies (Figure 4C and the SI);  $C_6F_5H$  has the highest value. Finally, extinction coefficients were measured at 450 nm for **1–3** in  $CH_2Cl_2$ , revealing that all three complexes absorb blue light with comparable efficiencies ( $\sim 20000$ – $25000$   $M^{-1} cm^{-1}$ ); given the high concentration of monomer in these reactions (2 M), we assume that the efficiency of monomer oxidation by **1–3** is comparable across S1–S6. The structural-, photophysical-, and reactivity-based similarities of **1–3** imply that only a very specific set of conditions is required for a deviation in the observed polymerization trends, which is, in turn, strongly suggestive of the WCA behavior of the monoanionic dodecaborate species following hole transfer to monomer.

**1** was also studied *in silico* in the presence of styrene substrate and explicit  $CH_2Cl_2$  solvent (see the SI for details). Several positions of styrene in close proximity to the  $-C_6F_5$  rings of **1** were identified, and time-dependent density functional theory (TD-DFT) calculations were then performed on the system at the B3LYP/6-31GS level of theory (Figure 5); the results are consistent with DFT calculations shown in Figure 4. Importantly, the donor molecular orbitals found in this simulation are positioned appropriately with respect to styrene to accept electron density following initiator photoexcitation, with some perturbation of the electronic structure observed at the  $-C_6F_5$  rings (given the presence of the styrene molecule) with respect to calculations shown in Figure 4.

Furthermore, the HOMO of the system is localized on styrene, again suggesting that ET from styrene upon cluster photoexcitation is mechanistically reasonable. Interestingly, when modeled in  $CH_3CN$ , both the HOMO and LUMO of the system are mostly located on the cluster core. This is consistent with our observation that  $<5\%$  polystyrene is generated under typical reaction conditions with **1** when  $CH_3CN$  is employed as the solvent.

While we have not been able to experimentally identify either substrate preorganization or the relative orientations of the styrene and initiator, as shown in Figure 5, they represent plausible modes of interaction by which ET may occur. However, it must also be noted that specific orientations are not required when invoking a tunneling mechanism for ET, which we suggest to be operative. It has been shown that electron tunneling can occur beyond 15 Å between the donor and acceptor even in the absence of covalent interactions;<sup>20</sup> while we have been unable to crystallographically characterize a donor–acceptor complex, the electron-self-exchange studies of **3** and  $[3]^-$  (vide supra) confirm that ET can occur even between dodecaborates, likely through tunneling. On the basis of the solid-state crystal structure of **3**, the closest *intermolecular* B–C or O–C

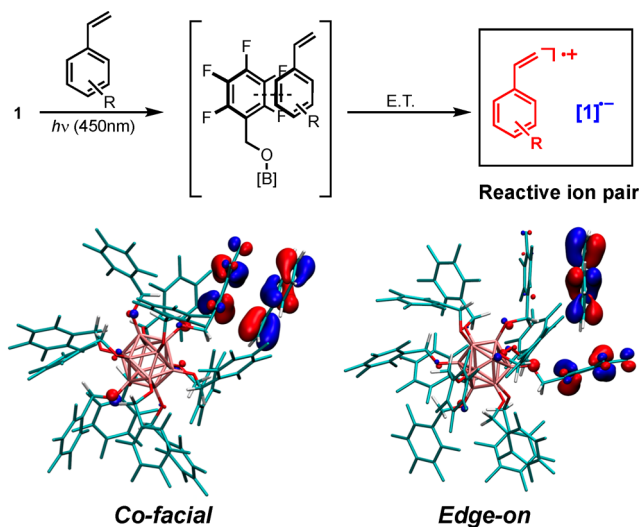


**Figure 5.** TD-DFT calculation of **1** in the presence of styrene (B3LYP/6-31GS). In-phase cofacial and edge-on dispositions of the styrene-based HOMO relative to a **1**-based molecular orbital suggest a possible pathway hole transfer to the substrate. Explicit  $CH_2Cl_2$  has been removed for clarity (see the SI for details).

distances (analogous to initiator–substrate distances) are well within 15 Å. Ultimately, these data indicate that the dodecaborane excited state<sup>21</sup> is quenched by very rapid hole transfer to the substrate.

## DISCUSSION OF PHOTOINITIATED POLYMERIZATION STUDIES

The above analyses suggest that the physical properties of the initiators, monomers, and media, *by themselves*, are likely not responsible for the anomalous  $M_n$  results but rather that a combination of properties, either prior to or during polymerization, accounts for the observed molecular weight differences. Nevertheless, this implies that **1** possesses a structural or electronic feature that is less prominent or absent in **2** and **3** or is potentially magnified to a greater degree than **2** or **3** in  $CH_2Cl_2$  in the presence of S2–S4. We turned to a time-point analysis of polymerizations conducted in the presence of **1** with various styrenes to further interrogate this system. The results are shown in Figure 6. The polymerizations of S1, S4, and S5

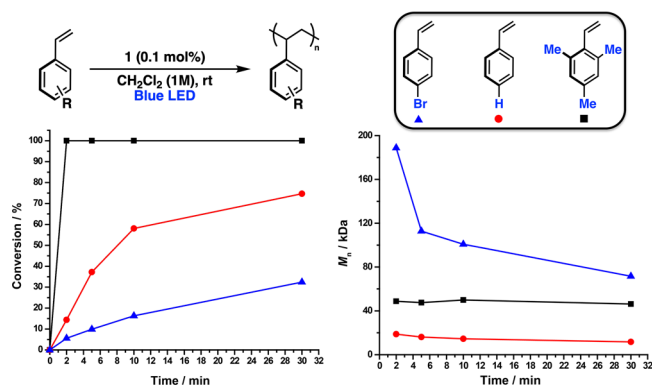


**Figure 6.** Polymerization of electronically diverse styrenes showing more rapid conversion for more electron-rich substrates but a higher initial  $M_n$  followed by a gradual decrease for S4 as opposed to those of S1 and S5, which remain constant during the reaction.

(1 M in  $\text{CH}_2\text{Cl}_2$ ) were initiated by **1** under blue-LED irradiation at room temperature. As expected, the rapidity of conversion scaled with the relative electron-richness of the monomer ( $\text{S5} > \text{S1} > \text{S4}$ ). Interestingly, gel permeation chromatography analysis of the same time points revealed that while the  $M_n$  values for poly-S1 and poly-S5 remained fairly consistent and low ( $\sim 20$  and  $\sim 50$  kDa, respectively) during the course of polymerization,  $M_n$  for poly-S4 began at  $\sim 190$  kDa and gradually decreased during the time frame in which aliquots were taken. This suggests that the ratio of the propagation rate to chain-transfer rate for S4 is fundamentally different from that for S1 and S5 and that this ratio reaches a steady state much later in the polymerization. This is potentially indicative of some additional factor (e.g., intermolecular interactions) that affects one or both terms of this ratio that is less prominent or absent with S1 and S5 under identical conditions. While we note that adventitious water can act as a powerful chain-transfer agent in carbocationic polymerizations, the clear dependence of  $M_n$  on the solvent and initiator suggests that the components of the reaction are more relevant to the observed polymer metrics.

The decay of  $M_n$  over time would be consistent with an increasing number of termination events relative to insertion events per time as the monomer depletes, particularly for an uncontrolled carbocationic polymerization of styrenes. While in photochemically initiated reactions, in particular, the initiator concentration is critical, we suggest that potential fluctuation in these values is not a dominant factor because only select polymers generated in the presence of **1** in  $\text{CH}_2\text{Cl}_2$  show high  $M_n$  values. Electron-withdrawing functional groups should render the  $\beta$ -proton of the propagating cationic chain more acidic than those in  $[\text{poly-S1}]^+$  or  $[\text{poly-S5}]^+$ , making it increasingly susceptible to loss of  $\text{H}^+$ . However, it is unclear why the  $M_n$  values for poly-S1 and poly-S5 do not also gradually decrease over time but instead remain constant during the course of the polymerization. The presence of poorly stabilized, free ion chain ends, which rapidly terminate, is consistent with this latter observation;<sup>22</sup> this scenario is analogous to decreased chain-end stabilization with decreasing solvent polarity, which also results in a larger number of chain-transfer events and lower-molecular-weight polymers in cationic polymerizations, as noted by Nuyken and co-workers.<sup>23</sup> Conversely, this also suggests that some degree of control, likely through more effective ion pairing, is imparted under the polymerization conditions of **1** and S4 in  $\text{CH}_2\text{Cl}_2$ ,

ultimately reducing chain transfer at early time points and giving rise to higher  $M_w$  values.

We find that the conversion of S1 in the presence of **1** in  $\text{CH}_2\text{Cl}_2$  is slower than that of 1,2-difluorobenzene. While according to Reichardt's  $E_T(30)$  scale,  $\text{CH}_2\text{Cl}_2$  and 1,2-difluorobenzene have comparable polarities,<sup>24</sup> this difference in the propagation rate has been observed in photoinitiated polymerizations of styrenes and isobutylene and has been attributed to differences in ion pairing as a result of varying medium polarity.<sup>22,25</sup> It was concluded in these cases that faster propagation resulted from free ions and slower propagation resulted from ion pairs. Furthermore, it was shown that free ions produced smaller  $M_n$  polymers than the ion pairs in these photoinitiated polymerizations. Interestingly, in the case of **1** and S4, we observe similar rates of conversion in both  $\text{CH}_2\text{Cl}_2$  and 1,2-difluorobenzene, while  $M_n$  of  $\text{CH}_2\text{Cl}_2$  at early time points reached up to  $\sim 190$  versus  $\sim 60$  kDa in 1,2-difluorobenzene under the same conditions (Figure 7). This

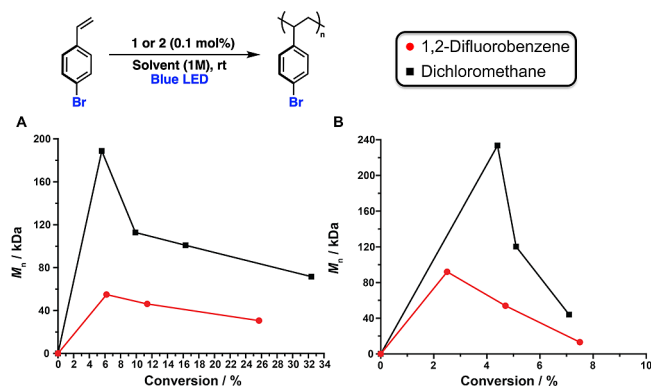


**Figure 7.**  $M_n$  versus conversion plots for the polymerization of S4 initiated by **1** (A) and **2** (B). While in both cases  $M_n$  starts at  $\sim 240$  kDa in  $\text{CH}_2\text{Cl}_2$ ,  $M_n$  decreases much more rapidly when initiated by **2**.

indicates that solvophobic effects similarly affect polymerizations of S4 by **1**, likely as a result of the strength of ion pairing of oligo- or poly-S4, specifically, with **1**. This result is consistent with the slightly higher dielectric constant of 1,2-difluorobenzene compared to  $\text{CH}_2\text{Cl}_2$ . To understand whether the similarity in the propagation rates was a function of the combination of S4 and **1** or dependent on S4 alone, we performed a similar set of experiments with **2** and S4. Here, we find that, in  $\text{CH}_2\text{Cl}_2$ , the initial  $M_n$  values at low conversion are high ( $\sim 240$  kDa) and gradually taper, whereas those in 1,2-difluorobenzene start much lower and likewise taper. Compared to **1** and S4, however,  $M_n$  drops much more rapidly as conversion increases. This suggests that S4 (and likely S2 and S3) exhibits similar behavior in the presence of **2** but that the proposed interactions are much less pronounced than those in the presence of **1**. Beyond solvophobic effects, it is also possible that 1,2-difluorobenzene materially interferes with ion pairing, particularly in the case of **1** and S2–S4 (vide infra).

Halide functional groups are capable of resonance stabilization of aromatic systems such that they behave as ortho- and para-directing substituents in electrophilic aromatic substitutions despite their inductively electron-withdrawing nature. Importantly, in these cases, the *position*, rather than simply the  $\pi$ -donating ability, of a halide substituent is critical in the observed reactivity and substitution pattern based on

canonical resonance forms that are available along the reaction coordinate. We considered that these substituents might be electronically stabilizing oligomeric or polymeric intermediates toward  $\beta$ -H<sup>+</sup> loss through resonance contributions, generating higher  $M_w$  fragments at early time points before chain transfer becomes more prominent as monomer depletes. Lenz and co-workers previously noted the potential importance of resonance effects of *p*-halide substituents in the carbocationic polymerization of *p*-*X*- $\alpha$ -methylstyrenes ( $X = \text{F}, \text{Cl}$ ).<sup>26</sup> Lewis et al. have also suggested this possibility.<sup>27</sup> While the presence and position of the halide in S2–S4 is clearly important, the consideration of resonance stabilization imparted by these functional groups still cannot explain the observation of high  $M_w$  in  $\text{CH}_2\text{Cl}_2$  with **1** only. Because there is a clear solvent effect on conversion (Figure 6) in which polymerization occurs more rapidly in 1,2-difluorobenzene versus  $\text{CH}_2\text{Cl}_2$  for S1 (see the SI), we posit that  $\text{CH}_2\text{Cl}_2$  favors a more tightly held ion pair between **1** and oligo- or poly-S2–S4, giving rise to polymers of high  $M_w$  and  $M_n$  for S2–S4. We suggest that the nature of this ion pair, in addition to the requisite electrostatic attraction, is through aromatic donor–acceptor interactions between the arene ring(s) of oligo- or poly-S2–S4 and the pentafluorophenyl substituents of **1** that are not present in **2** or **3**.

Intermolecular aromatic interactions have been widely observed<sup>28</sup> and used in the context of materials science,<sup>29</sup> molecular recognition,<sup>30</sup> biology,<sup>31</sup> and reaction chemistry.<sup>32</sup> Some of the most recognizable are those between electron-rich and (fluorinated) electron-poor aromatic rings ( $\text{Ar}^{\text{F}}$ ), which are believed to result, in part, from inversion of the electronic quadrupole of  $\text{Ar}^{\text{F}}$  relative to that of more electron-rich arenes, leading to favorable aromatic donor–acceptor interactions;<sup>33</sup> electrostatic, charge-transfer, and solvophobic effects have also been implicated in the facilitation of these aromatic interactions.<sup>34</sup> For example, in their study of interactions between  $\text{C}_6\text{F}_6$  and  $\text{C}_6\text{H}_5\text{X}$  arenes, Hunter and co-workers favored an electrostatic model of intermolecular arene interactions because of the linear correlation of the binding affinity with Hammett constants of substituted arene derivatives.<sup>35</sup> Gung and co-workers found deviations in this trend and also implicated significant charge-transfer effects in addition to electrostatic effects in order to fully explain the free energy of attraction between pentafluorobenzoate and 3,5-dinitrobenzoate groups with monofunctionalized arenes in a substituted triptycene manifold.<sup>36</sup> In addition, they posit that monosubstituted aryl rings as a donor–acceptor pair are not sufficiently electronically perturbed to engage in arene–arene interactions of meaningful magnitude; rather, electronic extremes such as  $-\text{C}_6\text{F}_5$  or  $-3,5-(\text{NO}_2)_2-\text{C}_6\text{H}_3$  moieties are necessary. Furthermore, Sherill and co-workers have shown that dispersion interactions can significantly contribute to the strength of the arene–arene interactions in face-to-face and edge-on arrangements of aryl rings.<sup>37</sup> The nonnegligible effect of the solvent on intermolecular interactions has been detailed,<sup>33b,38</sup> often in the context of effects on the electrostatic interactions or analyte desolvation. Finally, Cockroft and co-workers have also detailed the importance of *substituent* solvation in modulating the electrostatic potentials of aromatic systems.<sup>39</sup> While we cannot definitively identify the specific type of intermolecular interactions in the present case, based on our computational data of monomer interactions with **1** (see Figure 5) and the high local density of aryl substituents in **1**–**3** (particularly the  $-\text{C}_6\text{F}_5$  rings in **1**), electrostatic,

dispersion, charge-transfer, and solvophobic effects likely all contribute to the interactions of monomer with the ring periphery of the dodecaborate photoinitiators and are most prominent between S2 and S4 with **1** in  $\text{CH}_2\text{Cl}_2$ .<sup>40</sup>

Ion pairing under carbocationic polymerization conditions has historically been described through the Weinstein spectrum of ionicity<sup>25b</sup> and an associated equilibrium between dormant, contact ion pair, and fully solvated ions of a propagating cationic chain end and its corresponding anion. Biasing the equilibrium toward a contact ion pair through the addition of a “common ion”<sup>25b,41</sup> approximates the conditions under which controlled (“living”) carbocationic polymerization might be observed. We attempted to probe this equilibrium by employing readily accessible  $[\text{3}]^-$  as an additive in polymerizations initiated by **3**. If ion pairing is essential, one would expect that the addition of free  $[\text{3}]^-$  would drive the equilibrium toward a contact ion pair of propagating cationic polymer and counterion, giving rise to more controlled polymerizations with higher  $M_n$ .<sup>42</sup> The addition of S5 to a 1,2-difluorobenzene solution containing 0.1 mol % **3** and 0.1 mol %  $[\text{3}]^-$ , followed by blue-LED irradiation for 4 h and quenching with methanol, resulted in the expected precipitation of polymer. Upon workup, the isolated poly-S5 was found to display  $M_n$  values nearly double that obtained in the absence of  $[\text{3}]^-$  ( $M_n = 101$  vs 51.6 kDa; see the SI).

A similar experiment was conducted with S1 in 1,2-difluorobenzene, again revealing poly-S1 with approximately double the  $M_n$  relative to standard conditions (see the SI). Control polymerization experiments with  $[\text{3}]^-$  were performed and found not to initiate S1 polymerization under standard conditions, suggesting that **3** is completely responsible for the initial reactivity and oxidation of the styrene monomers. We also found that the addition of 0.1 mol %  $\text{NBu}_4\text{BARF}_4$ <sup>43</sup> to **3** and S1 under standard polymerization conditions in 1,2-difluorobenzene also resulted in polymers of increased molecular weight (Figure 8). Notably, increasing the amount of  $[\text{3}]^-$  in S1 polymerization experiments beyond 0.1 mol % does not result in a further increase of  $M_n$ . These experiments highlight the importance of ion-pair equilibria (Figure 9) in the resulting  $M_n$  and that, in comparison to **1** and S2–S4, the interactions between **2** or **3** and S2–S4 are significantly weaker in  $\text{CH}_2\text{Cl}_2$  and result in poly-S2–S4 of much lower  $M_n$ . The requirement of biasing these equilibria to observe higher  $M_n$  is consistent with the ionicity spectrum concept and the role of monoanionic **1**–**3** as WCAs.

In the carbocationic polymerization of styrene by  $\text{SnCl}_4$ , Overman and Newton observed that the addition of either durene or hexamethylbenzene resulted in an increase in  $M_n$  of the resulting polystyrene. They note: “No explanation of the atypical behavior of these methylbenzenes is readily apparent, but it is thought that there is a possibility that catalyst or catalyst-cocatalyst complexing with the aromatic compounds might affect the reaction when the aromatic compounds are as highly basic as these methylbenzenes.”<sup>44</sup> We wondered whether such complexation might involve interactions of durene with the propagating chain. We found that the addition of durene (1 equiv relative to **1**) to the polymerization of S1 by **1** under standard conditions only slightly increased the molecular weight of the resulting polymer (average 14 vs 8 kDa) but did not significantly alter the yield of the resulting polystyrene compared to the polymerization of styrene by **1** alone. While subtle, this  $M_n$  difference could implicate aromatic donor–acceptor interactions as operative in enhanc-

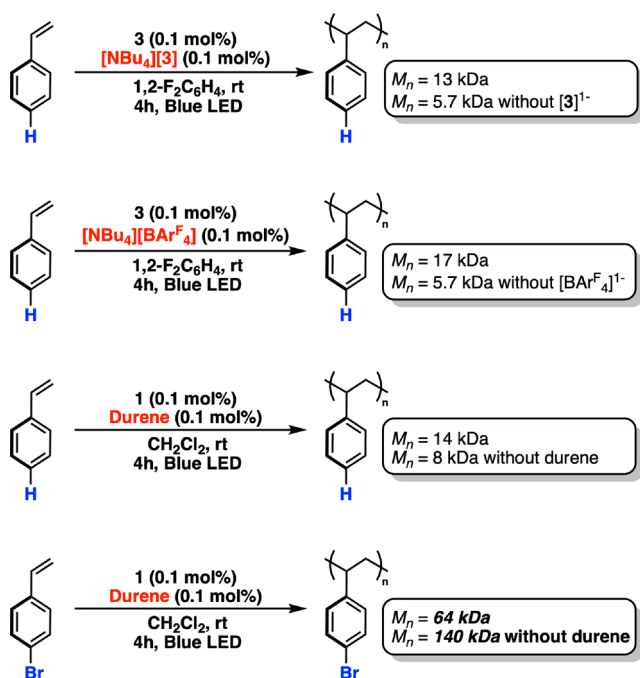


**Figure 8.** Control polymerization experiments by **1** and **3**, with select additives suggesting the importance of ion pairing in polymer molecular weights.

ing the  $M_n$  values; importantly, both durene and styrene are devoid of any Lewis basic substituents that might also be implicated as contributors to the  $M_n$  increase (vide supra). In an analogous reaction, durene (**1** equiv relative to **1**) was used as an additive in the polymerization of **S4** by **1**. In this case, we found that  $M_n$  and  $M_w$  were halved compared to poly-**S4** produced in the absence of durene, while the overall yield of the reaction was still comparable (Figure 8). This suggests that durene interferes with the reaction overall, either by reducing the rate of propagation on the time scale of chain transfer or by increasing the rate of chain transfer on the time scale of propagation. Given the discussion above, we suggest that durene competitively interacts with oligo- or poly-**S4** under the reaction conditions, preventing association with **1** and giving rise to lower  $M_w$ . We must also consider the possibility that similar interferences occur in the 1,2-difluorobenzene solvent, giving rise to low  $M_n$  for poly-**S2**–**S4** initiated by **1** in this medium. Overall, the specific reaction conditions required to generate the anomalous polymerization results obtained with **1** and the generally consistent results obtained in all other cases are indicative of the WCA behavior of  $[1]^- - [3]^-$ .

## CONCLUSION

Our work highlights the intricacies associated with the strength of ion-pairing interactions of the propagating cationic polymer

chain and a dodecaborate-based WCA as a function of the initiator, monomer, and solvent. Importantly, and despite the anomalous behavior of **1**, we can sterically and electronically diversify the dodecaborate proanions through the careful molecular design of the substituents appended onto the dodecaborate core to generate analogues such as **2** or **3**: these proanions still display strong photooxidizing potentials with nearly identical  $\lambda_{max}$ , molar absorptivities, and oscillator strengths for relevant visible-light transitions compared to **1**, and the monoanions generated through styrene oxidation appear devoid of significant intermolecular interactions with the cationic chain end. Charge-transfer excitation from the benzyloxy substituents to the cluster ultimately provides a driving force for ET from the olefin substrate. Furthermore, as a result of (1) the delocalization of unpaired electron density in these anions across the 12 boron atoms of the cage, (2) the cluster-based frontier molecular orbitals in both neutral and monoanionic ground states, and (3) the steric protection afforded by the organic substituents bound to each boron vertex of **1**–**3**, these WCAs remain chemically intact during the course of the cationic polymerization that occurs as a consequence of their photooxidizing ability. Overall, this supports the ability of  $[1]^- - [3]^-$  to behave as competent WCAs.

In our view, the photooxidative generation of  $[1]^- - [3]^-$ —akin to “redox-active  $[BAR_4]^-$ ” analogues—represents a fundamentally new approach to accessing WCAs, simply through visible-light irradiation. While there exist many visible-light photooxidants that have enjoyed steady use in the catalytic realm,<sup>45</sup> none possesses the extreme photooxidizing potentials displayed by **1**–**3**. While traditional  $BAR_4$ -based WCAs would be unstable toward oxidative coupling, the species presented here are themselves responsible for the oxidative strength and are compatible with these potentials. Ultimately, we envision the application of these and similar species<sup>46</sup> beyond polymer synthesis<sup>16,47</sup> to leverage the unique combination of a strong photooxidant and a WCA embodied in a single-cluster-based reagent, potentially providing access to otherwise inaccessible properties.

## ASSOCIATED CONTENT

### Supporting Information

The Supporting Information is available free of charge on the ACS Publications website at DOI: 10.1021/acs.inorgchem.9b00935.

Synthetic procedures and characterization, crystallographic information, computational parameters, absorption, and fluorescence spectroscopy (PDF)

Video of computations of styrene in the presence of **1** (MOV)

Video of computations of styrene in the presence of **1** (MOV)

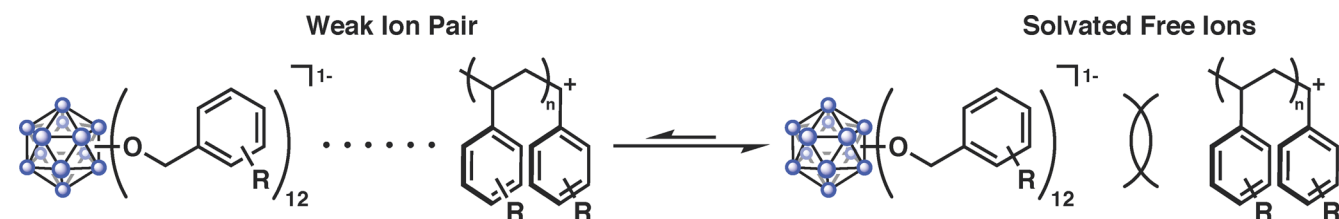


**Figure 9.** Proposed equilibrium between solvated and contact ion pairs between propagating polymer and dodecaborate WCAs **1**–**3**.

## Accession Codes

CCDC 1909003 contains the supplementary crystallographic data for this paper. These data can be obtained free of charge via [www.ccdc.cam.ac.uk/data\\_request/cif](http://www.ccdc.cam.ac.uk/data_request/cif), or by emailing [data\\_request@ccdc.cam.ac.uk](mailto:data_request@ccdc.cam.ac.uk), or by contacting The Cambridge Crystallographic Data Centre, 12 Union Road, Cambridge CB2 1EZ, UK; fax: +44 1223 336033.

## AUTHOR INFORMATION

## Corresponding Authors

\*E-mail: [axtell@ucla.edu](mailto:axtell@ucla.edu).

\*E-mail: [hbgray@caltech.edu](mailto:hbgray@caltech.edu).

\*E-mail: [pkral@uic.edu](mailto:pkral@uic.edu).

\*E-mail: [ana@chem.ucla.edu](mailto:ana@chem.ucla.edu).

\*E-mail: [spokorny@chem.ucla.edu](mailto:spokorny@chem.ucla.edu).

## ORCID

Jonathan C. Axtell: 0000-0002-5579-4296

Marco S. Messina: 0000-0003-2827-118X

Ji-Yuan Liu: 0000-0001-7905-6282

Daria Galaktionova: 0000-0003-2444-7168

Josef Schwan: 0000-0002-1086-6698

Tyler M. Porter: 0000-0002-2693-2653

Miles D. Savage: 0000-0002-6924-9360

Alex I. Wixtrom: 0000-0002-0622-4633

Arnold L. Rheingold: 0000-0003-4472-8127

Clifford P. Kubiak: 0000-0003-2186-488X

Jay R. Winkler: 0000-0002-4453-9716

Harry B. Gray: 0000-0002-7937-7876

Petr Král: 0000-0003-2992-9027

Anastassia N. Alexandrova: 0000-0002-3003-1911

Alexander M. Spokorny: 0000-0002-5683-6240

## Notes

The authors declare the following competing financial interest(s): UCLA holds patents on materials used in this work, from which A.M.S. may receive royalty payments.

## ACKNOWLEDGMENTS

The authors acknowledge Aayush Gupta (UIC) for preliminary computational work. M.S.M. was supported by NSF Bridge-to-Doctorate (Grant HRD-1400789) and Predoctoral Fellowship (Grant DGE-0707424) and the UCLA Christopher S. Foote Fellowship. H.B.G. was supported by the NSF (Grants CHE-1305124 and CHE-1763429). A.N.A. was supported by NSF CAREER Award CHE-1351968. Research pertaining to synthesis of the cluster compounds performed at UCLA was supported as part of the Synthetic Control Across Length-scales for Advancing Rechargeables (SCALAR) and Energy Frontier Research Center funded by the U.S. Department of Energy, Office of Science, Basic Energy Sciences, under Award DE-SC0019381. A.M.S. thanks 3M for a Non-Tenured Faculty Award, the Alfred P. Sloan Foundation for a Fellowship in Chemistry, and the Research Corporation for Science Advancement (RCSA) for a Cottrell Scholar Award. M.D.S. acknowledges a Dr. Raymond and Dorothy Wilson Research Fellowship (UCLA). A.I.W. acknowledges the University of California, Los Angeles, Graduate Division, for a Dissertation Year Fellowship.

## REFERENCES

(1) Yang, X.; Stern, C. L.; Marks, T. J. Cation-like" Homogeneous Olefin Polymerization Catalysts Based upon Zirconocene Alkyls and

Tris(pentafluorophenyl)borane. *J. Am. Chem. Soc.* **1991**, *113*, 3623–3625.

(2) Pellecchia, C.; Immirzi, A.; Grassi, A.; Zambelli, A. Base-Free Cationic Mono(cyclopentadienyl)zirconium Complexes: Synthesis, Structural Characterization, and Catalytic Activity in Olefin Polymerization. *Organometallics* **1993**, *12*, 4473–4478.

(3) (a) Shaffer, T. D.; Ashbaugh, J. R. Noncoordinating Anions in Carbocationic Polymerization. *J. Polym. Sci., Part A: Polym. Chem.* **1997**, *35*, 329–344. (b) Wang, Q.; Quyoum, R.; Gillis, D. J.; Tudoret, M.-J.; Jeremic, D.; Hunter, B. K.; Baird, M. C. Ethylene, Styrene, and  $\alpha$ -Methylstyrene Polymerization by Mono-(pentamethylcyclopentadienyl) ( $Cp^*$ ) Complexes of Titanium, Zirconium, and Hafnium: Roles of Cationic Complexes of the Type  $[Cp^*MR_2]^+$  ( $R = \text{Alkyl}$ ) as Both Coordination Polymerization Catalysts and Carbocationic Polymerization Initiators. *Organometallics* **1996**, *15*, 693–703. (c) Quyoum, R.; Wang, Q.; Tudoret, M.-J.; Baird, M. C.; Gillis, D. J.  $\eta^5$ - $C_5Me_5TiMe_3B(C_6F_5)_3$ : A Carbocationic Olefin Polymerization Initiator Masquerading as a Ziegler-Natta Catalyst. *J. Am. Chem. Soc.* **1994**, *116*, 6435–6436. (d) Wang, Q.; Baird, M. C. Carbocationic Initiation of Polymerization of Vinyl Ethers and *N*-Vinylcarbazole Induced by  $(\eta^5-C_5Me_5)TiMe_2(\mu-Me)-B(C_6F_5)_3$ . The First Examples of Polymerization of This Class of Electron-Rich Olefins by a Metallocene-like Initiator. *Macromolecules* **1995**, *28*, 8021–8027.

(4) (a) Crossing, I.; Reisinger, A. Chemistry with Weakly-Coordinating Fluorinated Alkoxyaluminate Anions: Gas Phase Cations in Condensed Phases? *Coord. Chem. Rev.* **2006**, *250*, 2721–2744. (b) Ewart, S. W.; Baird, M. C. Olefin Polymerization by Pentamethylcyclopentadienyl Trimethyltitanium,  $Cp^*TiMe_3$ . *Top. Catal.* **1999**, *7*, 1–8. (c) Bochmann, M. Kinetic and Mechanistic Aspects of Metallocene Polymerization Catalysts. *J. Organomet. Chem.* **2004**, *689*, 3982–3998. (d) Bochmann, M. The Chemistry of Catalyst Activation: The Case of Group 4 Polymerization Catalysts. *Organometallics* **2010**, *29*, 4711–4740. (e) Bochmann, M. Highly Electrophilic Organometallics for Carbocationic Polymerizations: From Anion Engineering to New Polymer Materials. *Acc. Chem. Res.* **2010**, *43*, 1267–1278. (f) Beck, W.; Sünkel, K. Metal Complexes of Weakly Coordinating Anions. Precursors of Strong Cationic Organometallic Lewis Acids. *Chem. Rev.* **1988**, *88*, 1405–1421.

(5) (a) Li, Y.; Cokoja, M.; Kühn, F. E. Inorganic/Organometallic Catalysts and Initiators Involving Weakly Coordinating Anions for Isobutene Polymerization. *Coord. Chem. Rev.* **2011**, *255*, 1541–1557. (b) LaPointe, R. E.; Roof, G. R.; Abboud, K. A.; Klosin, J. New Family of Weakly Coordinating Anions. *J. Am. Chem. Soc.* **2000**, *122*, 9560–9561. (c) Piers, W. E. The Chemistry of Perfluoroaryl Boranes. *Adv. Organomet. Chem.* **2004**, *52*, 1–76. (d) Pan, B.; Gabbai, F. P.  $[Sb(C_6F_5)_4][C(C_6F_5)_4]$ : An Air Stable, Lewis Acidic Stibonium Salt That Activates Strong Element-Fluorine Bonds. *J. Am. Chem. Soc.* **2014**, *136*, 9564–9567. (e) Johnson, A. M.; Contrella, N. D.; Sampson, J. R.; Zheng, M.; Jordan, R. F. Allosteric Effects in Ethylene Polymerization Catalysis. Enhancement of Performance of Phosphine-Phosphinate and Phosphine-Phosphonate Palladium Alkyl Catalysts by Remote Binding of  $B(C_6F_5)_3$ . *Organometallics* **2017**, *36*, 4990–5002. (f) Bernsdorf, A.; Brand, H.; Hellmann, R.; Köckerling, M.; Schulz, A.; Villinger, A.; Voss, K. Synthesis, Structure, and Bonding of Weakly Coordinating Anions Based on CN Adducts. *J. Am. Chem. Soc.* **2009**, *131*, 8958–8970. (g) Lancaster, S. J.; Walker, D. A.; Thornton-Pett, M.; Bochmann, M. New Weakly Coordinating Counter Anions for High Activity Polymerization Catalysts:  $[(C_6F_5)_3B-CN-B(C_6F_5)_3]^-$  and  $[Ni\{CNB(C_6F_5)_3\}_4]^{2-}$ . *Chem. Commun.* **1999**, 1533–1534. (h) Yin, Q.; Soltani, Y.; Melen, R. L.; Oestreich, M.  $BAr^F_3$ -Catalyzed Imine Hydroboration with Pinacolborane Not Requiring the Assistance of an Additional Lewis Base. *Organometallics* **2017**, *36*, 2381–2384. (i) Chen, E. Y.-X.; Marks, T. J. Cocatalysts for Metal-Catalyzed Olefin Polymerization: Activators, Activation Processes, and Structure-Activity Relationships. *Chem. Rev.* **2000**, *100*, 1391–1434. (j) Ghosh, S. K.; Ojeda, A. S.; Guerrero-Leal, J.; Bhuvanesh, N.; Gladysz, J. A. New Media for Classical Coordination Chemistry: Phase Transfer of Werner and Related Polycations into Highly



Nonpolar Fluorous Solvents. *Inorg. Chem.* **2013**, *52*, 9369–9378. (k) Riddlestone, I. M.; Kraft, A.; Schaefer, J.; Krossing, I. Taming the Cationic Beast: Novel Developments in the Synthesis and Application of Weakly Coordinating Anions. *Angew. Chem., Int. Ed.* **2018**, *57*, 13982–14024. (l) Klikovits, N.; Knaack, P.; Bomze, D.; Krossing, I.; Liska, R. Novel Photoacid Generators for Cationic Photopolymerization. *Polym. Chem.* **2017**, *8*, 4414–4421.

(6) (a) Tafazolian, H.; Culver, D. B.; Conley, M. P. A Well-Defined Ni(II)  $\alpha$ -Diimine Catalyst Supported on Sulfated Zirconia for Polymerization Catalysis. *Organometallics* **2017**, *36*, 2385–2388. (b) Stalzer, M. M.; Delferro, M.; Marks, T. J. Supported Single-Site Organometallic Catalysts for the Synthesis of High-Performance Polyolefins. *Catal. Lett.* **2015**, *145*, 3–14. (c) Ahn, H.; Marks, T. J. Supported Organometallics. Highly Electrophilic Cationic Metal-locene Hydrogenation and Polymerization Catalysts Formed via Protonolytic Chemisorption on Sulfated Zirconia. *J. Am. Chem. Soc.* **1998**, *120*, 13533–13534. (d) Williams, L. A.; Guo, N.; Motta, A.; Delferro, M.; Fragalà, I. L.; Miller, J. T.; Marks, T. J. Surface Structure-Chemical Characterization of a Single-Site  $d^0$  Heterogeneous Arene Hydrogenation Catalyst Having 100% Active Sites. *Proc. Natl. Acad. Sci. U. S. A.* **2013**, *110*, 413–418.

(7) (a) Weber, S. G.; Zahner, D.; Rominger, F.; Straub, B. F. A Cationic Gold Complex Cleaves  $BArF_4$ . *Chem. Commun.* **2012**, *48*, 11325–11327. (b) Salem, H.; Shimon, L. J. W.; Leitus, G.; Weiner, L.; Milstein, D. B–C Bond Cleavage of  $BArF_4$  Anion Upon Oxidation of Rhodium(I) with  $AgBArF_4$ . Phosphinite Rhodium(I), Rhodium(II), and Rhodium(III) Pincer Complexes. *Organometallics* **2008**, *27*, 2293–2299. (c) Konze, W. V.; Scott, B. L.; Kubas, G. J. First Example of B–C Bond Cleavage in the  $BArF_4$  ( $[B(C_6H_5)(CF_3)_2-3,5]_4$ ) Anion Mediated by a Transition Metal Species,  $trans$ - $[(PPh_3)_2Pt(Me)(OEt)]^+$ . *Chem. Commun.* **1999**, 1807–1808. (d) Bochmann, M.; Sarsfield, M. J. Reaction of  $AlR_3$  with  $[CPh_3][B(C_6F_5)_4]$ : Facile Degradation of  $[B(C_6F_5)_4]^-$  by Transient  $[AlR_2]^+$ . *Organometallics* **1998**, *17*, 5908–5912.

(8) For a study on borane adducts of water, see: (a) Bergquist, C.; Bridgewater, B. M.; Harlan, C. J.; Norton, J. R.; Friesner, R. A.; Parkin, G. Aqua, Alcohol, and Acetonitrile Adducts of Tris(perfluorophenyl)borane: Evaluation of Brønsted Acidity and Ligand Lability with Experimental and Computational Methods. *J. Am. Chem. Soc.* **2000**, *122*, 10581–10590. (b) Danopoulos, A. A.; Galsworthy, J. R.; Green, M. L. H.; Doerrer, L. H.; Cafferkey, S.; Hursthouse, M. Equilibria in the  $B(C_6F_5)_3 \cdot H_2O$  System: Synthesis and Crystal Structures of  $H_2O \cdot B(C_6F_5)_3$  and the Anions  $[HOB(C_6F_5)_3]^-$  and  $[(F_3C)_3B(\mu-OH) \cdot B(C_6F_5)_3]^-$ . *Chem. Commun.* **1998**, 2529–2560. (c) Doerrer, L. H.; Green, M. L. H. Oxidation of  $[M(\eta-C_5H_5)_2]$ ,  $M = Cr, Fe$  or  $Co$ , by the New Brønsted acid  $H_2O \cdot B(C_6F_5)_3$  Yielding the Salts  $[M(\eta-C_5H_5)_2]^+ A^-$ , where  $A = [(C_6F_5)_3B(\mu-OH)B(C_6F_5)_3]^-$  or  $[(C_6F_5)_3B \cdots H_2OB(C_6F_5)_3]^-$ . *J. Chem. Soc., Dalton Trans.* **1999**, 4325–4329.

(9) (a) Hewavitharanage, P.; Danilov, E. O.; Neckers, D. C. Pentafluorophenyl Transfer: A New Group-Transfer Reaction in Organoborate Salts. *J. Org. Chem.* **2005**, *70*, 10653–10659. (b) Kalamarides, H. A.; Iyer, S.; Lipian, J.; Rhodes, L. F.; Day, C. Pentafluoroaryl Transfer from Tris(pentafluorophenyl)boron Hydrate to Nickel. Synthesis and X-ray Crystal Structure of  $(PPh_2CH_2C(O)Ph)_2Ni(C_6F_5)_2$ . *Organometallics* **2000**, *19*, 3983–3990.

(10) (a) Beil, S. B.; Möhle, S.; Enders, P.; Waldvogel, S. R. Electrochemical Instability of Highly Fluorinated Tetraphenyl Borates and the Synthesis of their Respective Biphenyls. *Chem. Commun.* **2018**, *54*, 6128–6131. (b) Lawrence, E. J.; Oganessian, V. S.; Wildgoose, G. G.; Ashley, A. E. Exploring the Fate of the Tris(pentafluorophenyl)-borane Radical Anion in Weakly Coordinating Solvents. *Dalton Trans.* **2013**, *42*, 782–789. (c) Ashley, A. E.; Herrington, T. J.; Wildgoose, G. G.; Zaher, H.; Thompson, A. L.; Rees, N. H.; Krämer, T.; O'Hare, D. Separating Electrophilicity and Lewis Acidity: The Synthesis, Characterization, and Electrochemistry of the Electron Deficient Tris(aryl)boranes  $B(C_6F_5)_{3-n}(C_6Cl_5)_n$  ( $n = 1-3$ ). *J. Am. Chem. Soc.* **2011**, *133*, 14727–14740.

(11) Messina, M. S.; Axtell, J. C.; Wang, Y.; Chong, P.; Wixtrom, A. I.; Kirlikovali, K. O.; Upton, B. M.; Hunter, B. M.; Shafaat, O. S.; Khan, S. I.; Winkler, J. R.; Gray, H. B.; Alexandrova, A. N.; Maynard, H. D.; Spokoyny, A. M. Visible-Light-Induced Olefin Activation Using 3D Aromatic Boron-Rich Cluster Photooxidants. *J. Am. Chem. Soc.* **2016**, *138*, 6952–6955.

(12) (a) Gu, X.; Ozerov, O. V. Exhaustive Chlorination of  $[B_{12}H_{12}]^{2-}$  without Chlorine Gas and the Use of  $[B_{12}Cl_{12}]^{2-}$  as a Supporting Anion in Catalytic Hydrodefluorination of Aliphatic C–F Bonds. *Inorg. Chem.* **2011**, *50*, 2726–2728. (b) Wegener, M.; Huber, F.; Bolli, C.; Jenne, C.; Kirsch, S. F. Silver-Free Activation of Ligated Gold(I) Chlorides: The Use of  $[Me_3NB_{12}Cl_{11}]$  as a Weakly Coordinating Anion in Homogeneous Gold Catalysis. *Chem. - Eur. J.* **2015**, *21*, 1328–1336. (c) Kessler, M.; Knapp, C.; Zogaj, A. Cationic Dialkyl Metal Compounds of Group 13 Elements (E = Al, Ga, In) Stabilized by the Weakly Coordinating Dianion,  $[B_{12}Cl_{12}]^{2-}$ . *Organometallics* **2011**, *30*, 3786–3792. (d) Axtell, J. C.; Saleh, L. M. A.; Qian, E. A.; Wixtrom, A. I.; Spokoyny, A. M. Synthesis and Applications of Perfunctionalized Boron Clusters. *Inorg. Chem.* **2018**, *57*, 2333–2350.

(13) (a) Strauss, S. H. The Search for Larger and More Weakly Coordinating Anions. *Chem. Rev.* **1993**, *93*, 927–942. (b) Reed, C. A. Carboranes: A New Class of Weakly Coordinating Anions for Strong Electrophiles, Oxidants, and Superacids. *Acc. Chem. Res.* **1998**, *31*, 133–139. (c) Douvris, C.; Michl, J. Update 1 of: Chemistry of the Carba-closo-dodecaborate(–) Anion,  $CB_{11}H_{12}^-$ . *Chem. Rev.* **2013**, *113*, PR179–PR233. (d) Douvris, C.; Ozerov, O. V. Hydrodefluorination of Perfluoroalkyl Groups Using Silylium-Carborane Catalysts. *Science* **2008**, *321*, 1188–1190. (e) Nava, M. J.; Reed, C. A. High Yield C-Derivatization of Weakly Coordinating Carborane Anions. *Inorg. Chem.* **2010**, *49*, 4726–4728. (f) Dziedzic, R. M.; Waddington, M. A.; Lee, S. E.; Kleinsasser, J.; Plumley, J. B.; Ewing, W. C.; Bosley, B. D.; Lavallo, V.; Peng, T. L.; Spokoyny, A. M. Reversible Silver Electrodeposition from Boron Cluster Ionic Liquid (BCIL) Electrolytes. *ACS Appl. Mater. Interfaces* **2018**, *10*, 6825–6830. (g) Krossing, I.; Raabe, I. Noncoordinating Anions – Fact or Fiction? A Survey of Likely Candidates. *Angew. Chem., Int. Ed.* **2004**, *43*, 2066–2090. (h) Reed, C. A.  $H^+$ ,  $CH_3^+$ , and  $R_3Si^+$  Carborane Reagents: When Triflates Fail. *Acc. Chem. Res.* **2010**, *43*, 121–128. (i) Kitazawa, Y.; Takita, R.; Yoshida, K.; Muranaka, A.; Matsubara, S.; Uchiyama, M. Naked<sup>+</sup> Lithium Cation: Strongly Activated Metal Cations Facilitated by Carborane Anions. *J. Org. Chem.* **2017**, *82*, 1931–1935. (j) Ivanov, S. V.; Peryshkov, D. V.; Miller, S. M.; Anderson, O. P.; Rappé, A. K.; Strauss, S. H. Synthesis, Structure, and Reactivity of  $AlMe_2(1-Me-CB_{11}F_{11})$ . An  $AlMe_2^+$  Cation-like Species Bonded to a Superweak Anion. *J. Fluorine Chem.* **2012**, *143*, 99–102. (k) Fisher, S. P.; Tomich, A. W.; Lovera, S. O.; Kleinsasser, J. F.; Guo, J.; Asay, M. J.; Nelson, H. M.; Lavallo, V. Nonclassical Applications of closo-Carborane Anions: From Main Group Chemistry and Catalysis to Energy Storage. *Chem. Rev.* **2019**, DOI: 10.1021/acs.chemrev.8b00551.

(14) (a) Popov, S.; Shao, B.; Bagdasarian, A. L.; Benton, T. R.; Zou, L.; Yang, Z.; Houk, K. N.; Nelson, H. M. Teaching an Old Carbocation New Tricks: Intermolecular C–H Insertion Reactions of Vinyl Cations. *Science* **2018**, *361*, 381–387. (b) Shao, B.; Bagdasarian, A. L.; Popov, S.; Nelson, H. M. Arylation of Hydrocarbons Enabled by Organosilicon Reagents and Weakly Coordinating Anions. *Science* **2017**, *355*, 1403–1407.

(15) Wixtrom, A. I.; Shao, Y.; Jung, D.; Machan, C. W.; Kevork, S. N.; Qian, E. A.; Axtell, J. C.; Khan, S. I.; Kubiak, C. P.; Spokoyny, A. M. Rapid Synthesis of Redox-Active Dodecaborane  $B_{12}(OR)_{12}$  Clusters under Ambient Conditions. *Inorg. Chem. Front.* **2016**, *3*, 711–717.

(16) Aubry, T. J.; Axtell, J. C.; Basile, V. M.; Winchell, K. J.; Lindemuth, J. R.; Porter, T. M.; Liu, J.-Y.; Alexandrova, A. N.; Kubiak, C. P.; Tolbert, S. H.; Spokoyny, A. M.; Schwartz, B. J. Dodecaborane-Based Dopants Designed to Shield Anion Electrostatics Lead to Increased Carrier Capacity in a Doped Conjugated Polymer. *Adv. Mater.* **2019**, *31*, 1805647.

- (17) (a) Goeltz, J. C.; Hanson, C. J.; Kubiak, C. P. Rates of Electron Self-Exchange Reactions between Oxo-Centered Ruthenium Clusters Are Determined by Orbital Overlap. *Inorg. Chem.* **2009**, *48*, 4763–4767. (b) Goeltz, J. C.; Benson, E. E.; Kubiak, C. P. Electronic Structural Effects in Self-Exchange Reactions. *J. Phys. Chem. B* **2010**, *114*, 14729–14734. (c) Porter, T. M.; Canzi, G. C.; Chabolla, S. A.; Kubiak, C. P. Tuning Electron Delocalization and Transfer Rates in Mixed-Valent Ru3O Complexes through “Push–Pull” Effects. *J. Phys. Chem. A* **2016**, *120*, 6309–6316.
- (18) (a) Kanazawa, A.; Shibutani, S.; Yoshinari, N.; Konno, T.; Kanaoka, S.; Aoshima, S. Structure Effects of Lewis Acids on the Living Cationic Polymerization of *p*-Methoxystyrene: Discinct Difference in Polymerization Behavior from Vinyl Ethers. *Macromolecules* **2012**, *45*, 7749–7757. Note: Initial studies revealed that the polymerizations proceeded in the presence of atmospheric oxygen as well as radical traps (see ref 11). Inhibition of SS polymerization by **1** in the presence of 2,6-<sup>t</sup>Bu<sub>2</sub>-C<sub>6</sub>H<sub>3</sub>N was also observed, indicating the importance of H<sup>+</sup> in chain termination/reinitiation, which is common in uncontrolled carbocationic polymerizations. In addition, the cationic polymerization originating from cation radicals has been studied. For example, see: (b) Pilar, J.; Marek, M.; Toman, L. The Formation of Radical Cations of Styrene and  $\alpha$ -Methylstyrene in the Irradiation of Mixtures of These Monomers with TiCl<sub>4</sub> and SnCl<sub>4</sub> in a Semicrystalline Heptane Matrix. *J. Polym. Sci., Polym. Chem. Ed.* **1980**, *18*, 3193–3197. (c) Akbulut, U.; Fernandez, J. E.; Birke, R. L. Electroinitiated Cationic Polymerization of Styrene by Direct Electron Transfer. *J. Polym. Sci., Polym. Chem. Ed.* **1975**, *13*, 133–149. (d) Sparapany, J. J. Ion–Molecule Reactions in Liquid Hydrocarbons via Photoionization with Vacuum Ultraviolet Radiation. The Polymerization of Isobutene. *J. Am. Chem. Soc.* **1966**, *88*, 1357–1362. (e) Michaudel, Q.; Kottisch, V.; Fors, B. P. Cationic Polymerization: From Photoinitiation to Photocontrol. *Angew. Chem., Int. Ed.* **2017**, *56*, 9670–9679.
- (19) Hansch, C.; Leo, A.; Taft, R. W. A Survey of Hammett Substituent Constants and Resonance and Field Parameters. *Chem. Rev.* **1991**, *91*, 165–195.
- (20) Wenger, O. S.; Leigh, B. S.; Villahermosa, R. M.; Gray, H. B.; Winkler, J. R. Electron Tunneling Through Organic Molecules in Frozen Glasses. *Science* **2005**, *307*, 99–102.
- (21) Boeré, R. T.; Derendorf, J.; Jenne, C.; Kacprzak, S.; Keßler, M.; Riebau, R.; Riedel, S.; Roemmele, T. L.; Rühle, M.; Scherer, H.; Vent-Schmidt, T.; Warneke, J.; Weber, S. On the Oxidation of the Three-Dimensional Aromatics [B<sub>12</sub>X<sub>12</sub>]<sup>2-</sup> (X = F, Cl, Br, I). *Chem. - Eur. J.* **2014**, *20*, 4447–4459.
- (22) Yamamoto, Y.; Irie, M.; Hayashi, K. Photoinduced Ionic Polymerization. VI. Molecular Weight Distribution in Cationic Polymerization of  $\alpha$ -Methylstyrene. *Polym. J.* **1976**, *8*, 437–441.
- (23) Vierle, M.; Zhang, Y.; Santos, A. M.; Köhler, K.; Haeßner, C.; Herdtweck, E.; Bohnenpoll, M.; Nuyken, O.; Kühn, F. E. Solvent-Ligated Manganese(II) Complexes for the Homopolymerization of Isobutene and the Copolymerization of Isobutene and Isoprene. *Chem. - Eur. J.* **2004**, *10*, 6323–6332.
- (24) Reichardt, C. Solvatochromic Dyes as Solvent Polarity Indicators. *Chem. Rev.* **1994**, *94*, 2319–2358.
- (25) (a) Suzuki, M.; Yamamoto, Y.; Irie, M.; Hayashi, K. Polymerization of Styrene Initiated By Photoexcited Charge-Transfer Complex. *J. Macromol. Sci., Chem.* **1976**, *10*, 1607–1622. (b) Perneckner, T.; Kennedy, J. P. Living Carbocationic Polymerization. XLVI. Living Isobutylene Polymerization Induced by the Common Ion Effect. *Polym. Bull.* **1991**, *26*, 305–312.
- (26) (a) Lenz, R. W.; Faullimel, J. G.; Jonte, J. M.; Fisher, D. J. Characterization of the Active Centers in the Cationic Polymerization of *p*-Substituted  $\alpha$ -Methylstyrenes. *Makromol. Chem., Macromol. Symp.* **1988**, *13-14*, 255–269. (b) Lenz, R. W.; Fisher, D. J.; Jonte, J. M. Cationic Polymerization of Para-Substituted  $\alpha$ -Methylstyrenes. 6. Solvent Polarity Effects on Polymer Tacticity. *Macromolecules* **1985**, *18*, 1659–1663.
- (27) Lewis, M.; Bagwill, C.; Hardebeck, L. K. E.; Wireduah, S. The Use of Hammett Constants to Understand the Non-Covalent Binding of Aromatics. *Comput. Struct. Biotechnol. J.* **2012**, *1*, e201204004.
- (28) Meyer, E. A.; Castellano, R. K.; Diederich, F. Interactions with Aromatic Rings in Chemical and Biological Recognition. *Angew. Chem., Int. Ed.* **2003**, *42*, 1210–1250.
- (29) (a) Shao, S.; Hu, J.; Wang, X.; Wang, L.; Jing, X.; Wang, F. Blue Thermally Activated Delayed Fluorescence Polymers with Non-conjugated Backbone and Through-Space Charge Transfer Effect. *J. Am. Chem. Soc.* **2017**, *139*, 17739–17742. (b) Sun, L.; Campbell, M. G.; Dinca, M. Electrically Conductive Porous Metal-Organic Frameworks. *Angew. Chem., Int. Ed.* **2016**, *55*, 3566–3579. (c) Yao, Z.-F.; Wang, J.-Y.; Pei, J. Control of  $\pi$ - $\pi$  Stacking via Crystal Engineering in Organic Conjugated Small Molecule Crystals. *Cryst. Growth Des.* **2018**, *18*, 7–15.
- (30) (a) Cozzi, F.; Ponzini, F.; Annunziata, R.; Cinquini, M.; Siegel, J. S. Polar Interactions between Stacked  $\pi$  Systems in Fluorinated 1,8-Diarylnaphthalenes: Importance of Quadrupole Moments in Molecular Recognition. *Angew. Chem., Int. Ed. Engl.* **1995**, *34*, 1019–1020. (b) Salonen, L. M.; Ellermann, M.; Diederich, F. Aromatic Rings in Chemical and Biological Recognition: Energetics and Structures. *Angew. Chem., Int. Ed.* **2011**, *50*, 4808–4842.
- (31) (a) Patrick, C. R.; Prosser, G. S. A Molecular Complex of Benzene and Hexafluorobenzene. *Nature* **1960**, *187*, 1021. (b) Burley, S. K.; Petsko, G. A. Aromatic-Aromatic Interaction: A Mechanism of Protein Structure Stabilization. *Science* **1985**, *229*, 23–28. (c) Pace, C. J.; Gao, J. Exploring and Exploiting Polar- $\pi$  Interactions with Polar Aromatic Amino Acids. *Acc. Chem. Res.* **2013**, *46*, 907–915.
- (32) (a) Coates, G. W.; Dunn, A. R.; Henling, L. M.; Dougherty, D. A.; Grubbs, R. H. Phenyl–Pentafluorophenyl Stacking Interactions: A New Strategy for Supermolecule Construction. *Angew. Chem., Int. Ed. Engl.* **1997**, *36*, 248–251. (b) Senaweera, S.; Weaver, J. D. S<sub>N</sub>Ar Catalysis Enhanced by an Aromatic Donor-Acceptor Interaction; Facile Access to Chlorinated Polyfluoroarenes. *Chem. Commun.* **2017**, *53*, 7545–7548.
- (33) (a) Williams, J. H.; Cockcroft, J. K.; Fitch, A. N. Structure of the Lowest Temperature Phase of the Solid Benzene–Hexafluorobenzene Adduct. *Angew. Chem., Int. Ed. Engl.* **1992**, *31*, 1655–1657. (b) Martinez, C. R.; Iverson, B. L. Rethinking the Term “ $\pi$ -Stacking”. *Chem. Sci.* **2012**, *3*, 2191–2201. (c) Grimme, S. Do Special Noncovalent  $\pi$ - $\pi$  Stacking Interactions Really Exist? *Angew. Chem., Int. Ed.* **2008**, *47*, 3430–3434.
- (34) (a) Ringer, A. L.; Sherrill, C. D. Substituents Effects in Sandwich Configurations of Multiply Substituted Benzene Dimers Are Not Solely Governed by Electrostatic Control. *J. Am. Chem. Soc.* **2009**, *131*, 4574–4575. (b) Meyer, E. A.; Castellano, R. K.; Diederich, F. Interactions with Aromatic Rings in Chemical and Biological Recognition. *Angew. Chem., Int. Ed.* **2003**, *42*, 1210–1250. (c) Hunter, C. A.; Sanders, J. K. M. The Nature of  $\pi$ - $\pi$  Interactions. *J. Am. Chem. Soc.* **1990**, *112*, 5525–5534. (d) Hwang, J. w.; Li, P.; Shimizu, K. D. Synergy Between Experimental and Computational Studies of Aromatic Stacking Interactions. *Org. Biomol. Chem.* **2017**, *15*, 1554–1564.
- (35) Cockcroft, S. L.; Hunter, C. A.; Lawson, K. R.; Perkins, J.; Urch, C. J. Electrostatic Control of Aromatic Stacking Interactions. *J. Am. Chem. Soc.* **2005**, *127*, 8594–8595.
- (36) (a) Gung, B. W.; Patel, M.; Xue, X. A Threshold for Charge Transfer in Aromatic Interactions? A Quantitative Study of  $\pi$ -Stacking Interactions. *J. Org. Chem.* **2005**, *70*, 10532–10537. (b) Gung, B. W.; Amicangelo, J. C. Substituent Effects in C<sub>6</sub>F<sub>6</sub>-C<sub>6</sub>H<sub>5</sub>X Stacking Interactions. *J. Org. Chem.* **2006**, *71*, 9261–9270.
- (37) (a) Ringer, A. L.; Sinnokrot, M. O.; Lively, R. P.; Sherrill, C. D. The Effect of Multiple Substituents on Sandwich and T-Shaped  $\pi$ - $\pi$  Interactions. *Chem. - Eur. J.* **2006**, *12*, 3821–3828. (b) Sinnokrot, M. O.; Sherrill, C. D. Unexpected Substituent Effects in Face-to-Face  $\pi$ -Stacking Interactions. *J. Phys. Chem. A* **2003**, *107*, 8377–8379.
- (38) (a) Smithrud, D. B.; Diederich, F. Strength of Molecular Complexation of Apolar Solutes in water and in Organic Solvents Is Predictable by Linear Free Energy Relationships: A General Model

for Solvation Effects on Apolar Binding. *J. Am. Chem. Soc.* **1990**, *112*, 339–343. (b) Chapman, K. T.; Still, W. C. A Remarkable Effect of Solvent Size on the Stability of a Molecular Complex. *J. Am. Chem. Soc.* **1989**, *111*, 3075–3077. (c) Canceill, J.; Lacombe, L.; Collet, A. A New Cryptophane Forming Unusually Stable Inclusion Complexes with Neutral Guests in a Lipophilic Solvent. *J. Am. Chem. Soc.* **1986**, *108*, 4230–4232.

(39) Muchowska, K. B.; Adam, C.; Mati, I. K.; Cockroft, S. L. Electrostatic Modulation of Aromatic Rings via Explicit Solvation of Substituents. *J. Am. Chem. Soc.* **2013**, *135*, 9976–9979.

(40) For additional discussions of intermolecular aromatic interactions, see: (a) Sinnokrot, M. O.; Sherrill, C. D. Substituent Effects in  $\pi - \pi$  Interactions: Sandwich and T-Shaped Configurations. *J. Am. Chem. Soc.* **2004**, *126*, 7690–7697. (b) Paliwal, S.; Geib, S.; Wilcox, C. S. Molecular Torsion Balance for Weak Molecular Recognition Forces. Effects of “Tilted-T” Edge-to-Face Aromatic Interactions on Conformational Selection and Solid-State Structure. *J. Am. Chem. Soc.* **1994**, *116*, 4497–4498. (c) Kim, E.-I.; Paliwal, S.; Wilcox, C. S. Measurements of Molecular Electrostatic Field Effects in Edge-to-Face Aromatic Interactions and CH- $\pi$  Interactions with implications for Protein Folding and Molecular Recognition. *J. Am. Chem. Soc.* **1998**, *120*, 11192–11193. (d) Nishio, M.; Umezawa, Y.; Hirota, M.; Takeuchi, Y. The CH/ $\pi$  Interaction: Significance in Molecular Recognition. *Tetrahedron* **1995**, *51*, 8665–8701. (e) Yang, L.; Adam, C.; Nichol, G. S.; Cockroft, S. L. How Much do van der Waal Dispersion Forces Contribute to Molecular Recognition in Solution? *Nat. Chem.* **2013**, *5*, 1006–1010. (f) Cockroft, S. L.; Hunter, C. A. Desolvation Tips the Balance: Solvent Effects on Aromatic Interactions. *Chem. Commun.* **2006**, 3806–3808.

(41) (a) Nagy, A.; Majoros, I.; Kennedy, J. P. Living Carbocationic Polymerization. LXII. Living Polymerization of Styrene, *p*-Methylstyrene and *p*-Chlorostyrene Induced by the Common Ion Effect. *J. Polym. Sci., Part A: Polym. Chem.* **1997**, *35*, 3341–3347. (b) Higashimura, T.; Ishihama, Y.; Sawamoto, M. Living Cationic Polymerization of Styrene: New Initiating Systems Based on Added Halide Salts and the Nature of the Growing Species. *Macromolecules* **1993**, *26*, 744–751.

(42) Higashimura, T.; Aoshima, S.; Sawamoto, M. New Initiators for Living Cationic Polymerization of Vinyl Compounds. *Makromol. Chem., Macromol. Symp.* **1988**, *13-14*, 457–471.

(43) (a) Nishida, H.; Takada, N.; Yoshimura, M.; Sonoda, T.; Kobayashi, H. Tetrakis[3,5-bis(trifluoromethyl)phenyl]borate. Highly Lipophilic Stable Anionic Agent for Solvent-extraction of Cations. *Bull. Chem. Soc. Jpn.* **1984**, *57*, 2600–2604. (b) Hill, M. G.; Lamanna, W. M.; Mann, K. R. Tetrabutylammonium Tetrakis[3,5-bis-(trifluoromethyl)phenyl]borate as a Noncoordinating Electrolyte: Reversible  $1e^-$  Oxidations of Ruthenocene, Osmocene, and  $Rh_2(TM4)_4^{2+}$  ( $TM4 = 2,5$ -Diisocyno-2,5-dimethylhexane). *Inorg. Chem.* **1991**, *30*, 4687–4690.

(44) Overberger, C. G.; Newton, M. G. Ionic Polymerization. XV. Further Molecular Terminating Agents in the Cationic Polymerization of Styrene. *J. Am. Chem. Soc.* **1960**, *82*, 3622–3626.

(45) (a) Prier, C. K.; Rankic, D. A.; MacMillan, D. W. C. Visible Light Photoredox Catalysis with Transition Metal Complexes: Applications in Organic Synthesis. *Chem. Rev.* **2013**, *113*, 5322–5363. (b) Narayanam, J. M. R.; Stephenson, C. R. J. Visible Light Photoredox Catalysis: Applications in Organic Synthesis. *Chem. Soc. Rev.* **2011**, *40*, 102–113. (c) Du, Y.; Pearson, R. M.; Lim, C. H.; Sartor, S. M.; Ryan, M. D.; Yang, H.; Damrauer, N. H.; Miyake, G. M. Strongly Reducing Visible Light Organic Photoredox Catalysts as Sustainable Alternatives to Precious Metals. *Chem. - Eur. J.* **2017**, *23*, 10962–10968.

(46) (a) Wixtrom, A. I.; Parvez, Z.; Savage, M. A.; Qian, E. A.; Jung, D.; Khan, S. I.; Rheingold, A. L.; Spokoyny, A. M. Tuning the Electrochemical Potential of Perfunctionalized Dodecaborate Clusters Through Vertex Differentiation. *Chem. Commun.* **2018**, *54*, 5867–5870. (b) Axtell, J. C.; Kirlikovali, K. O.; Jung, D.; Dzedzic, R. M.; Rheingold, A. L.; Spokoyny, A. M. Metal-Free Peralkylation of the *closo*-Hexaborate Anion. *Organometallics* **2017**, *36*, 1204–1210.

(47) Jung, D.; Saleh, L. M. A.; Berkson, Z. J.; El-Kady, M. F.; Hwang, J. Y.; Mohamed, N.; Wixtrom, A. I.; Titarenko, E.; Shao, Y.; McCarthy, K.; Guo, J.; Martini, I. B.; Kraemer, S.; Wegener, E. C.; Saint-Cricq, P.; Ruehle, B.; Langeslay, R. R.; Delferro, M.; Brosmer, J. L.; Hendon, C. H.; Gallagher-Jones, M.; Rodriguez, J.; Chapman, K. W.; Miller, J. T.; Duan, X.; Kaner, R. B.; Zink, J. I.; Chmelka, B. F.; Spokoyny, A. M. A Molecular Cross-Linking Approach for Hybrid Metal Oxides. *Nat. Mater.* **2018**, *17*, 341–348.